

Localization and Target Tracking of Marine Vessels Exploiting Miscellany of Multi-Global Positioning System Signals for High Frequency Surface Wave Radar

Abstract

Rapidly localizing, detecting and tracking group targets effectually on sea surface requires effective tracking system approach. This paper utilizes techniques of Global Positioning system with wave radar to identify, sort and track sea targets. The radar takes initial scan on sea surface to acquire the DBS image and quickly, the image get processed by the Constant false alarm rate to detect the targets on the sea. In accordance with the numerous parameters dispense by the Inertia Navigation System, the station connection linking the radar and a precise target can be obtained. The radar places the servomechanism system to enable the antenna to ray the targets location which permits the radar to hurriedly advance to mono pulse tracking. The outcomes reveal that, the suggested system and algorithm is capable of localizing, sort group targets, speedily and progressively track precise targets. The implementation of the technique presented in this paper is highly appropriate for missile field.

Introduction

In recent decades, much attention has been pondered on the employment and consideration of High Frequency Surface Wave Radar to be a powerful expedient for long range sensing device in marine remote sensing implementations [1]. It operates in frequency range of about 4-30MHz and can pose a novel way for vigorous, unrelenting, and instantaneous detection and tracking of poignant marine vessel targets afar the skyline. However, there are some disadvantages associated with the usage of High Frequency Surface Wave Radar for target tracking and localization; these include short range and the resolution of azimuth that lead to inaccurate target locations, which permits the attained track diverge from its precise stations; meddling, clutter end up in deficiency of target contacts for some period of time leading to track disintegration and diminutions its aptitude for tenacious tracking. These imperfections make it cumbersome to yield high quality tracks for High Frequency Surface Wave Radar and rim its implementations in maritime surveillance [2]. To solve these glitches; a potent and appropriate algorithm need to be constructed to overawed these precincts; on the other hand, previous studies indicate that, it is very knotty for a High Frequency Surface Wave Radar to function in lone frequency means, single-handedly to gain highest excellence tracks, other

Open Access

Review Article

Samuel Acquah^{*1}, Mark Owusu Adjei², Anastasia Krampah-Nkoom³

¹Mechatronics & Automation Engineering Department, Shanghai University, China

²College of Landscape Architecture, Plant Science, Sichuan Agriculture University, China


³School of Management and Business Administration, Jiangsu University, China

*Address for Correspondence

Samuel Acquah, Mechatronics & Automation Engineering Department, Shanghai University, China

Submission: June 19, 2020

Published: June 29, 2020

Copyright: ©  This work is licensed under Creative Commons Attribution 4.0 License

idea from the target should be achieved to sustain the tracking technique, and knowledge centered target tracking has been attractive as possible and auspicious tendency [3]. The auxiliary knowledge of the vis-à-vis target can be originated from other radar positions in a multi-station network surveillance system [4], also it can be attained from other revealing means, such as the Automatic Identification System. Further, the impression can also be achieved from a High Frequency Surface Wave Radar itself via dual- or multi-frequency function way [5]. A High Frequency Surface Wave Radar employs absolute separated electromagnetic waves for target detection and tracking, it classically functions at the lesser end of High Frequency band to yield from minor superficial wave attenuation rates hence advances the detection dependability and assortment [6]. To assuage the target obscurity triggered by Bragg peaks and the magnitude of ionospheric disorder, a High Frequency Surface Wave Radar can be premeditated to function promptly at dual further frequencies [7]. Nevertheless, High Frequency spectrum is hugely teemed, it is used by radios, noncombatant and martial long range communications, etc. The lesser the frequency is, the starker the spectrum excess becomes. Also, as the number of the working frequencies intensify, the intricacies and the hardware outlays rise melodramatically. Henceforth dual or multi frequency is a good trade-off [8].

In dealing with the trajectory disintegration concern triggered by absent target contacts through nearly epoch due to the sea clutter, the scholar constructed innovative vessel target tracking technique that takes the benefit of the frequency multiplicity possessions of a dual-frequency High Frequency Surface Wave Radar, which can work in dual frequencies concomitantly [9]. In this method, the target data from dual frequencies are chronologically assimilated together to enhance the tracking importunity competences. The paper is arranged as follows: The second section focuses on the proposed algorithm for High Frequency Surface Wave Radar target detection and tracking; the third section defines the proposed technique in detail; the

forth section concentrate on the Tracking experimental results and discussions while section 5 ends the study with the conclusion.

Preliminaries

High Frequency Surface Wave Radars are well-thought-out as comprehensible devices, they distinguish amid reverberations incipient from superficial vessels and the usually more prevailing ocean resonance through their variance in Doppler shifts. The radar is installed on the motorial podium and its antenna probes the imaging zones under the control of the servo system and then the radar’s signal processor can take the resonances to image.

The radar transmitter chirp signals when scanning for the target. As an example to the point target, its reverberation expression is:

$$s(p_r, p) = A_r \left(p_r - \frac{2R_p}{c} \right) A_a(p) e^{j\pi k_r \left(p_r - \frac{2R_p}{c} \right)^2} e^{j2\pi f_0 \left(p - \frac{2R_p}{c} \right)} \tag{1}$$

In afore written equation, denotes the range window function while represents azimuth window function. Connotes the real time incline distance and is the signal speed. Is the hauler frequency and is the assortment period and P is the total period and c is the swiftness of light. To obtain the real ricochet signal, the hauler frequency could be done away with to get

$$s(p_r, p) = A_r \left(p_r - \frac{2R_p}{c} \right) A_a(p) e^{j\pi k_r \left(p_r - \frac{2R_p}{c} \right)^2} e^{j2\pi f_0 \left(p - \frac{2R_p}{c} \right)} e^{-j4\pi/\lambda R_p} \tag{2}$$

Here, the assortment looseness is excepted and the equivalent function is computed as

$$s_{r_p} (p_r) = a_r (p_r) e^{-j\pi k_r p_r^2} \tag{3}$$

After the compression, the expression becomes

$$s(p_r, p_m) = IFFP(FFP[S(P_r, p_m)].FFP[s_{r_p}(p_r)]) \\ = A_{a_a} (p_a) \sin c \left(\Delta B_r \left(p_r - \frac{2R_r}{c} \right) \right) e^{-j4\pi/\lambda R_r} \tag{4}$$

In the above equation, A implies the amplitude of the signal, denotes the bandwidth of the signal, hence;

$$R_p \approx R_0 - vt \sin \theta \cos \phi \tag{5}$$

In the eq5, θ represents scan angle and R_0 is the original diagonal distance and v is the speed of the platform and ϕ is the plunging angle. For Eq. 5, it can be deduced that, walk rectification should be calculated by using rectification factor procedure to burgeon the signal in the range frequency dominion. The expression for the rectification factor is:

$$H_f = e^{-j4\pi v p \sin \theta \cos \phi / c f_r} \tag{6}$$

Here, the walk rectification is kaput and the Doppler centroid is appraised via fractional signal to complete the Doppler center recompense. Multi-look meting out and azimuth FFT is computed to acquire the child image of the sight. Full DBS image can be achieved by coalescing the child image and regulating the topographical synchronizes. Below is the flow of the algorithm.

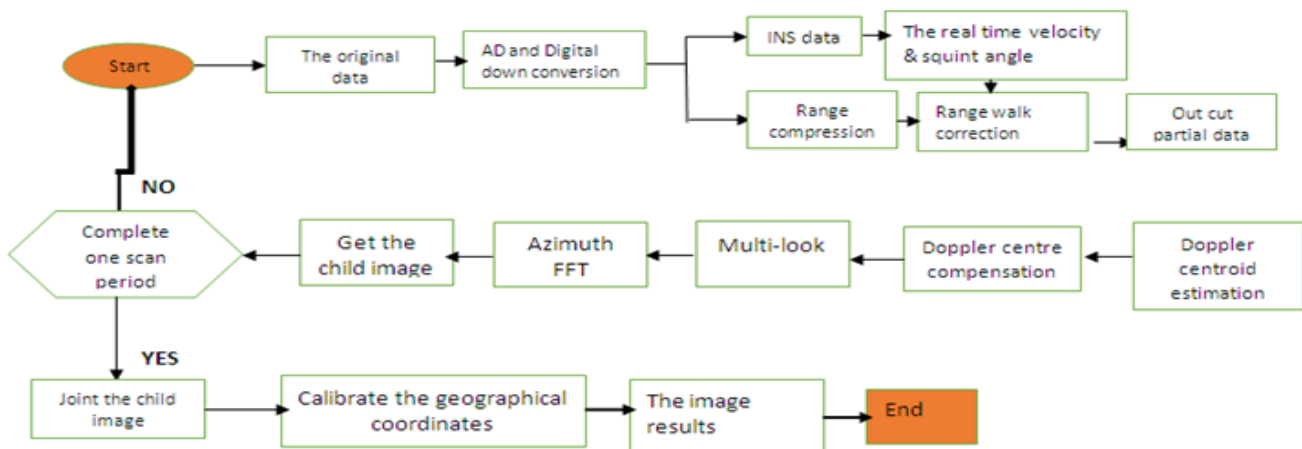


Figure 1: The procedure of DBS imaging algorithm

Target Localization And Detection

Upon acquisition of DBS image, target detection is computed by exploiting advanced OSCA-CFAR algorithm. OS-CFAR is utilized in array province and CA-CFAR in Doppler realm to augment the brink localization and detection enactment and the precision of multi-targets detection. Under the unvarying Rayleigh envelope clutter conditions, OSCA-CFAR detector uses a square-detector to process the data of DBS image to obtain the squared amplitude of the data and then carries through a data withdrawal in series domain and Doppler domain. Then the detector uses a sliding window to achieve a detection verge.

The expression for the detection threshold of CA-CFAR is computed as

$$P_{CA} = \alpha_{CA} \cdot \mu_{CA} \tag{7}$$

$$\mu_{CA} = \frac{1}{M \times N} \sum_{i=1}^M \cdot \sum_{j=1}^N \chi_{ij} \tag{8}$$

In the above equations implies the detector factor of CA-CFAR where M and N denote row number and column number of data in the window respectively. Defines the intensity value for the element.

The detection verge for the OS-CFAR indicator is given as

$$P_{OS} = \alpha_{OS} \cdot X(k) \tag{9}$$

For α_{OS} stands for the OS-CFAR indicator factor and $X(k)$ means the value of Kth intensity of the element when the value of the intensity is in ascending order; $X(1) < X(2) < \dots < X(k) < \dots < X(M \cdot N)$

The k's value is gritty by the average level of noise. The detection verge of the OSCA-CFAR detector is dogged by the principle of detection brink of the CA-CFAR detector and OS-CFAR detector. First ly, apiece range data is arranged in soaring order, and then the mean value of the Doppler data is to be solved based on the value of k. Finally the detection brink is attained as follows.

$$P_{OSCA} = \alpha_{OSCA} \cdot \mu_{OSCA} \tag{10}$$

$$\mu_{OSCA} = \frac{1}{N} \sum_{j=1}^N \chi_{(k)j} \tag{11}$$

Here, α_{OSCA} is a factor of the OSCA-CFAR detector and $\chi_{(k)j}$ represents value for the intensity of the kth Doppler data which is being fixed already. Further, for the experiential formula, α_{OSCA} it can be written as follows.

$$\alpha_{OSCA} = \frac{-\ln(P_{fa})}{\sum_{j=1}^k \frac{1}{N - k + j}} \tag{12}$$

For the equation above, P_{fa} stands for the likelihood of the invalid alarm, by this technique, accurate detection verge matrix to do the judgement of statistics could be obtained. In normalcy, a lot of the targets on the sea are in solitary. In order to enhance the efficiency of computation, prior to using the OSCA-CFAR indicator. We firstly utilized global verge to assess the whole image. All the algorithm is demonstrated below.

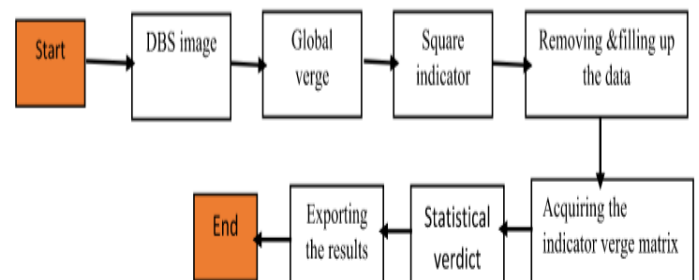


Figure 2: The tide of the OSCA-CFAR algorithm.

Rapid Target Tracking

On completing the image detection, the target region could easily be known and exact target can be picked to track according to the ethics. To foster the adeptness, we utilize Global Positioning System plus Inertial Navigation System to work coordinates objectives out. Here, servomechanism is then set hastily to enable the antenna to swiftly radiate the target estimated area so that the radar can track the precise target. The rapid procedure for tracking precise target is skillfully designed below.

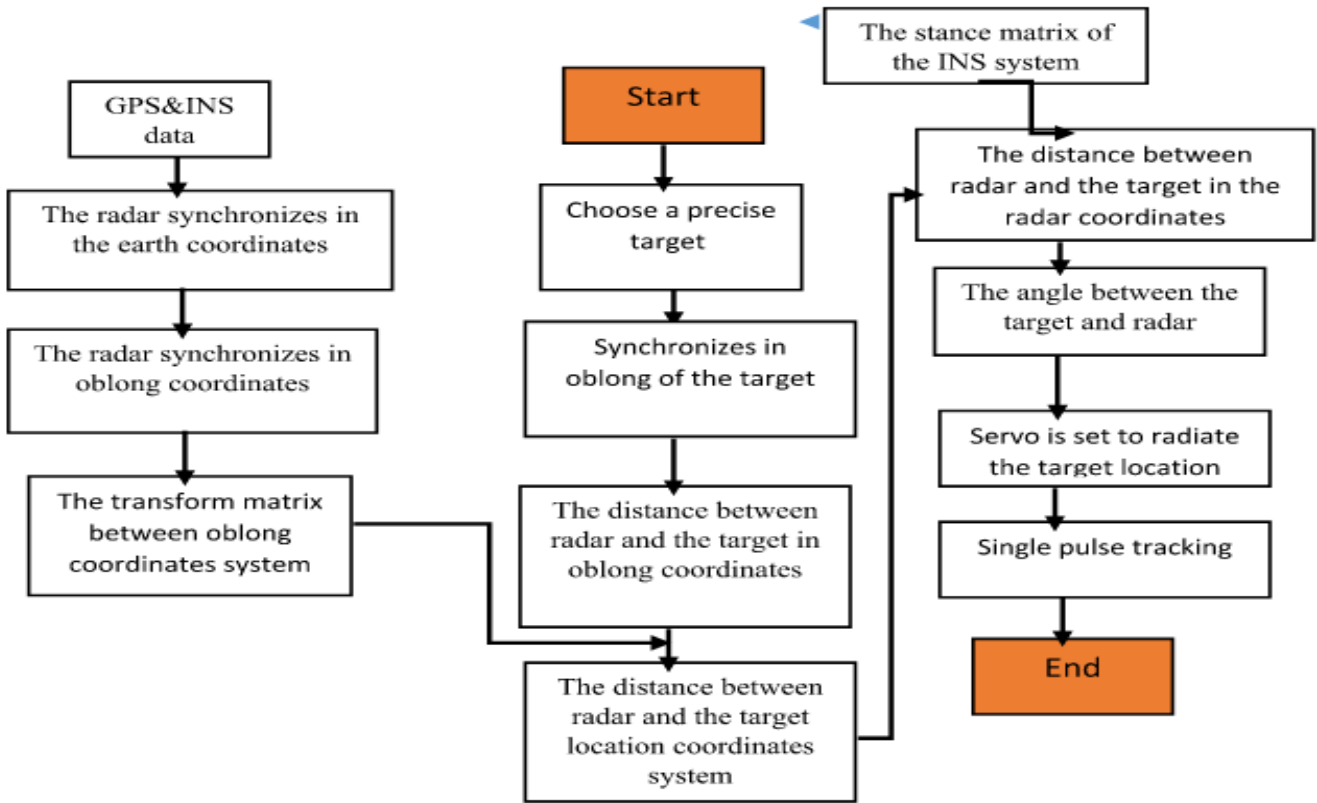


Figure 3: Rapid tide of tracking precise target.

Supposing that M_s denotes the radar's location of latitude and N_s represents longitude where H_s is radar's height. M_t Signifies the target's station, N_t is the longitude and H_t stands for the height of the target. R_e Stands for the semi-major axis of the earth and e defines the earth's ovality, in that arc radius of the earth at where both the target and the radar situated can be expressed independently as:

$$R_s = R_e \cdot (1 + e^{\sin(N_s)})^2 \quad (13)$$

$$R_t = R_e \cdot (1 + e^{\sin(N_t)})^2 \quad (14)$$

Initially, we ably changed the spherical coordinate's perpendicular to the quadrilateral coordinates system at the place both radar and target are situated. (a_s, b_s, c_s) Denotes the target's quadrilateral coordinates and (a_t, b_t, c_t) represents the quadrilateral coordinates of the target, more specifically,

$$a_s = (R_s + N_s) \cos(M_s) \cos(s_s) \quad (15)$$

$$b_s = (R_s + N_s) \cos(M_s) \sin(s_s) \quad (16)$$

$$c_s = (R_s(1 - e)^2 + H_s) \sin(N_s) \quad (17)$$

$$a_t = (R_t + M_t) \cos(M_t) \cos(s_t) \quad (18)$$

$$b_t = (R_t + M_t) \cos(M_t) \sin(s_t) \quad (19)$$

$$c_t = (R_t(1 - e)^2 + H_t) \sin(N_t) \quad (20)$$

Here, we skillfully computed the distance amid the radar and the target in the system's coordinate of the quadrilateral.

$$a_{st} = a_s - a_t \quad (21)$$

$$b_{st} = b_s - y_t \quad (22)$$

$$c_{st} = c_s - c_t \quad (23)$$

Afterwards, we rehabilitated the fissure from the coordinate of the quadrilateral system to the terrestrial coordinate system and mathematically, the switched matrix can be written as:

$$B = \begin{bmatrix} B_{11} & B_{12} & B_{13} \\ B_{21} & B_{22} & B_{23} \\ B_{31} & B_{32} & B_{33} \end{bmatrix} = \begin{bmatrix} -\sin(s_s) \cos(S_s) 0 \\ -\sin(N_s) \cos(s_s) - \sin(N_s) \sin(S_s) \cos(N_s) \\ \cos(N_s) \cos(S_s) \cos(N_s) \sin(S_s) \sin(N_s) \end{bmatrix} \tag{24}$$

From the above equation, the interval in the terrestrial coordinate system can be written as:

$$\begin{bmatrix} D_{n_e} \\ D_{n_n} \\ D_{n_s} \end{bmatrix} = \begin{bmatrix} B_{11} & B_{12} & B_{13} \\ B_{21} & B_{22} & B_{23} \\ B_{31} & B_{32} & B_{33} \end{bmatrix} \begin{bmatrix} a_{st} \\ b_{st} \\ c_{st} \end{bmatrix} = \begin{bmatrix} a_{st} B_{11} + b_{st} B_{12} + c_{st} B_{13} \\ a_{st} B_{21} + b_{st} B_{22} + c_{st} B_{23} \\ a_{st} B_{31} + b_{st} B_{32} + c_{st} B_{33} \end{bmatrix} \tag{25}$$

In equation (25), D_{n_e} denotes the interval in the east and D_{n_n} represents the interval in the north whilst D_{n_s} signifies the array in the route of the height. Hence the posture matrix of the INS system can be computed as:

$$C = \begin{bmatrix} C_{11} & C_{12} & C_{13} \\ C_{21} & C_{22} & C_{23} \\ C_{31} & C_{32} & C_{33} \end{bmatrix} = \begin{bmatrix} \cos \gamma \cos \alpha + -\cos \gamma \sin \alpha + \\ \sin \gamma \sin \alpha \sin \beta \sin \gamma \cos \alpha \sin \beta - \sin \gamma \cos \beta \\ \sin \alpha \cos \beta \cos \alpha \cos \beta \sin \beta \\ \sin \gamma \cos \alpha - -\sin \gamma \sin \alpha - \cos \gamma \cos \beta \\ \cos \gamma \sin \alpha \sin \beta \cos \gamma \cos \alpha \sin \beta \end{bmatrix} \tag{26}$$

In equation (26), α implies the slant of direction obtain from the Inertia Navigation System and β is the pitching slant where γ also represents the undulating angle, so the actual distance among the radar and the target in the coordinate system of the topographical place can be rehabilitated to the distance in the radar coordinate system. Mathematically, it can be expressed as:

$$\begin{bmatrix} A_c \\ B_c \\ C_c \end{bmatrix} = \begin{bmatrix} C_{11} & C_{12} & C_{13} \\ C_{21} & C_{22} & C_{23} \\ C_{31} & C_{32} & C_{33} \end{bmatrix} \begin{bmatrix} D_{n_e} \\ D_{n_n} \\ D_{n_s} \end{bmatrix} = \begin{bmatrix} D_{n_e} C_{11} + D_{n_n} C_{12} + D_{n_s} C_{13} \\ D_{n_e} C_{21} + D_{n_n} C_{22} + D_{n_s} C_{23} \\ D_{n_e} C_{31} + D_{n_n} C_{32} + D_{n_s} C_{33} \end{bmatrix} \tag{27}$$

Here, A_c , B_c and C_c imply the interval in thrice archetypal guidelines. In that, the incline amid the radar and the target can be acquired in triple directions in the radar coordinate system. In this way, we are able to compute the actual angle which the servomechanism must be set to enable the radar's antenna to point to the target devoid of error. In arranging servomechanism, the coordinates of the targets in the radar coordinates system must be estimated and computed. With this notion, we are able to achieve the information of radar's servo system and its positon in the image of the DBS. This enabled us to technically utilized equation (15) & equation (27) to get the target coordinates in the radar coordinate system. The procedure is skillfully designed below.

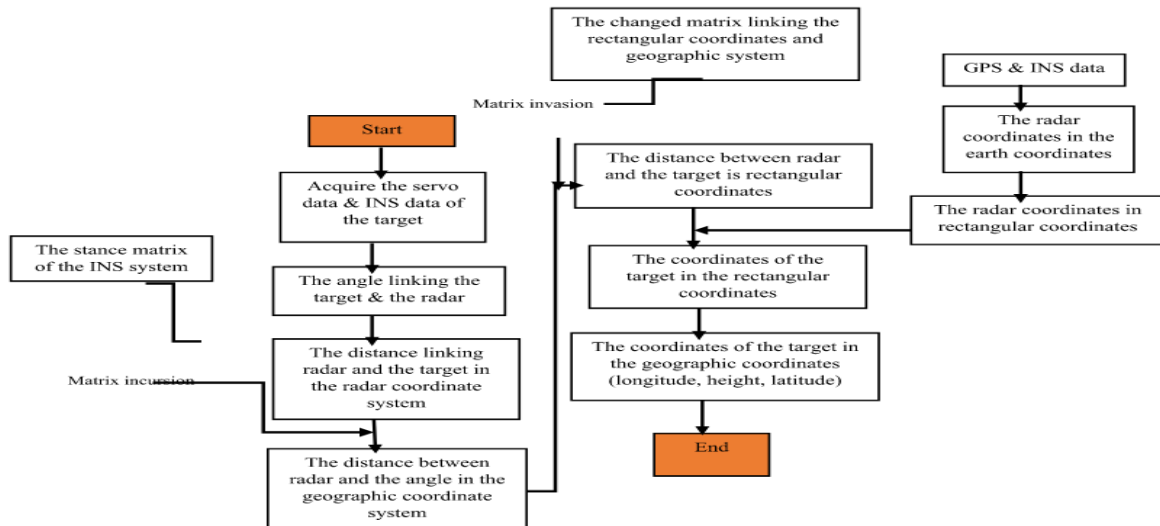


Figure 4: the procedure of computing the coordinates of the system.

With this systematic technique, we can trace the precise target rapidly by DBS imaging, image detection and setting the servomechanism system.

result is clearly demonstrated in figure 6 with main target tagged with identification numbers. The results proved to be very accurate with the target originally set.

Authentication of The Proposed Algorithm

In this study, the investigational data was ably derived from flight test. The rapidity was estimated to be approximately 70.5 meters per seconds. The route of the flight is assumed to be skewed at a confident angle from the targets location. The radar is however, placed under the plane. The radiation orientation of the antenna is consistent with the flight path and direction of the Inertia Navigation system. In the location of the targets, there were four mini boats distanced from each other of about 5010 meters. The radar is switched on when the aircraft stands about 76km away from the target location and then commence to process the image. The outcome of the DBS image is shown below.

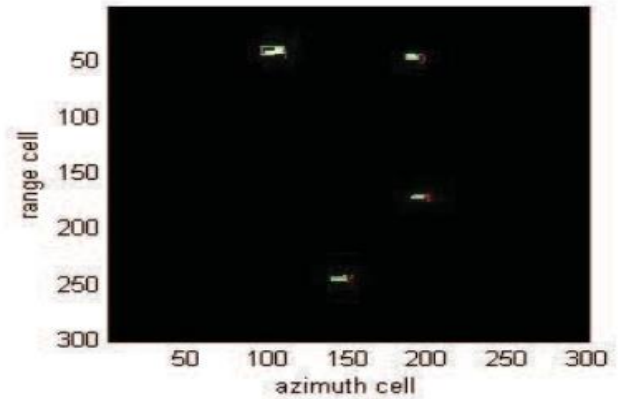


Figure 6: Results of the Constant False Alarm Rate (CFAR)

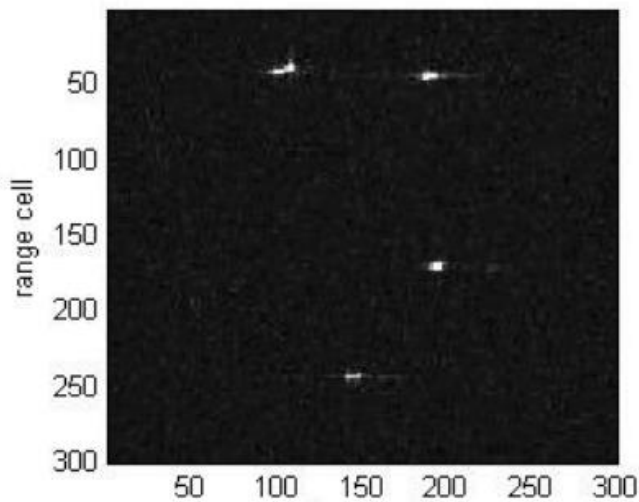


Figure 5: four targets can be seen here, the image is administered by the enhanced OSCA-CFAR algorithm. The

In the process, we chose second target to track according to the ethics of tracking the closest. The entire result of this study is vividly illustrated in figure 7. In this result, we demonstrated the angle of azimuth for the servomechanism system, the angle of the pitch for the servo system, the distance between the Radio Detection and Ranging, second target and tracking sign that “0” shows no stating of tracking and “1” denotes tracking state. Where the tracking sign reaches zero, the distance between the radar and the second target gets to “0”. It can be inferred from the azimuth angle of servo system, the radar initially scans the location of the target with an approximate angle of 5 degrees Celsius to 30 degrees Celsius with servo being held at the current position where the signal processor of the radar computes as illustrated above. Finally, the servo system is set with the radar to execute the mono pulse tracking. In clear view from figure 7, the scanning cost for DBS stands five seconds and the while the other computations described above stands ten seconds.

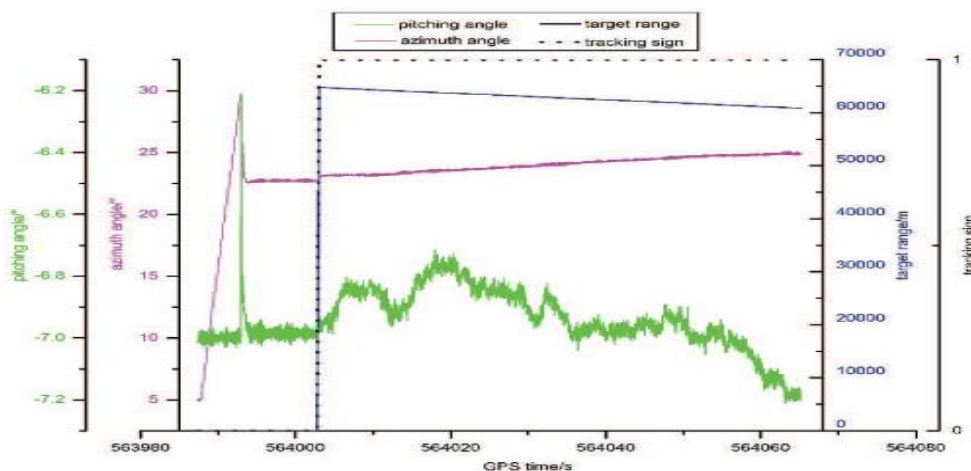


Figure 7: Experimental result

The results of the test proves that the presented algorithm is capable of completing the detection and able to locate targets of marine vessels and track precise target hastily. The time that the radar costs from scanning the sea surface to tracking a specific target is just 16 seconds, so this algorithm has high implementation competences.

Conclusion Remarks

With the upsurge growth of the marine technology, localization and target tracking has become imperative and concern for many countries to pay much attention to identifying, detecting and tracking targets at sea. The results of this paper has high significant contribution to the field of military surveillance as the propose algorithm is able to detect and determine the target's location within shortest possible time. The results of the algorithm prove to be very powerful with high accuracy and operational efficiency. The algorithm presented in this paper has high application prospect in the field of locating, detecting and tracking targets on the sea.

References

1. Wyatt LR (2014) High frequency radar applications in coastal monitoring, planning and engineering. *J Aus Civil Eng* 12: 1-15.
2. Melnikova A, Sivagurunathana K, Guoa X, Toleva J, Mandelis A, et al., (2017) Non-destructive thermal-wave-radar imaging of manufactured green powder metallurgy compact flaws (cracks) *NDT & E Int* 86: 140-152.
3. Salimi H (2015) Stochastic fractal search: A powerful metaheuristic algorithm. *Knowladge based system* 75: 1-18.
4. Wang F, Xu F, Jin YQ (2017) Simulation of multi-station ISAR imaging for monitoring a space target: A case of Envisat. *IEEE International Geoscience and Remote Sensing Symposium (IGARSS)*.
5. Sun W, Dai Y, Ji Y, Zhou P, Won Y (2016) Vessel target tracking exploiting frequency diversity for dual-frequency HFSWR. in 2016 CIE International Conference on Radar (RADAR). *IEEE*.
6. Chen S, Gill EW, Huang (2016) A first-order HF radar cross-section model for mixed-path ionosphere-ocean propagation with an FMCW source. 41: 982-992.
7. Headrick JM, Thomason JF (1998) Applications of high-frequency radar 33: 1045-1054.
8. Li Z, Pradeep GK, Deng Y, Raabe D, Tasan CC, et al., (2016) Metastable high-entropy dual-phase alloys overcome the strength-ductility trade-off 534: 227-230.
9. Liu Y, Bucknall R (2015) Path planning algorithm for unmanned surface vehicle formations in a practical maritime environment. *Ocean Eng* 126-144.

Assets of Publishing with us

Global archiving of articles
 Immediate, unrestricted
 online access Rigorous Peer
 Review Process Authors
 Retain Copyrights

<https://www.biomedress.com>

Submission Link: <https://biomedress.com/online-submission.php>